Defect and Diffusion Forum
ISSN: 1662-9507, Vol. 452, pp 59-64
doi:10.4028/p-h1jN4u
© 2026 The Author(s). Published by Trans Tech Publications Ltd, Switzerland.
Submitted: 2025-09-27
Revised: 2025-12-19
Accepted: 2026-02-23
Online: 2026-05-18

High Quality P-Type 4H-SiC Growth by PVT Method

Shanshan Hu[1,a*], Haochi Wang[1,b], Zeyu Chen[1,c], Kaixuan Zhang[1,d], Yuzhuo Li[1,e], Jianpei Zhang[1,f], Balaji Raghothamachar[1,g], Michael Dudley[1,h], Douglas Dukes[2,i] and Victor Torres[2,j]

[1]Department of Materials Science & Chemical Engineering, Stony Brook University, Stony Brook, NY 11794, USA

[2]Pallidus, Inc., Albany, NY 12203, USA

[a*]shanshan.hu@stonybrook.com, [b]haochi.wang@stonybrook.edu, [c]zeyu.chen@stonybrook.edu, [d]kaixuan.zhang@stonybrook.edu, [e]yuzhuo.li@stonybrook.edu, [f]jianpei.zhang@stonybrook.edu, [g]balaji.raghothamachar@stonybrook.edu, [h]michael.dudley@stonybrook.edu, [i]douglas.dukes@pallidus.com, [j]victor.torres@pallidus.com

Keywords: 4H-SiC, p-type, PVT growth.

Abstract. The fabrication of n-channel IGBTs is constrained by the low conductivity as well as poor quality of the p-type SiC substrate. This paper reports a 6-inch high quality p-type 4H-SiC wafer achieved by PVT method. The wafer was examined by synchrotron X-ray topography indicating average defect densities are on par or better than commercial 6-inch n-type wafers. Large areas of the wafer, especially the middle region of the wafer is characterized by very low density of BPDs. The extent of prismatic slip due to radial thermal gradients is also vastly reduced compared to typical n-type wafers.

Introduction

With outstanding electronic properties such as high breakdown field strength, high operating temperatures, high thermal conductivity, and high carrier saturation drift velocity, silicon carbide (SiC) is becoming the choice for fabrication of high-power electronic devices. Various device types such as diodes (JBS, SBD, PiN) and transistors (MOSFET, JFET, IGBT) have been developed chiefly on n-doped substrates. Among these, the SiC insulated gate bipolar transistors (IGBTs) have demonstrated great performance advantages and application prospects as high-voltage switches. Especially, n-channel IGBTs show superior performance than p-channel IGBTs due to higher mobility of electrons than holes but fabrication is preferable on p-doped substrates.

However, the fabrication of n-channel IGBTs is constrained by the low conductivity as well as poor quality of the p-type SiC substrate [1], which is essential for their device performance. Usually, p-type SiC is manufactured using an aluminum (Al)-containing compound placed in the SiC powder region as dopant. Since the vapor pressure of Al is significantly higher than that of the SiC gas species during crystal growth, the Al source is released excessively in the early stage of crystal growth and gets depleted for the later growth stage. As a result, it is hard to achieve stable and continuous p-type doping. In addition, the high concentration of Al at the seed/newly grown crystal interface affects the crystallization quality and leads to large defect nucleation. So far, Suo et al. [2] achieved 3-inch N-Al co-doped p-type SiC crystals with regions having BPD etch pit density of 300 cm^{-2}. 4-inch p-type 4H-SiC is obtained by Wang et al. [3] with dislocation etching pit density of 888.89 cm^{-2}. Compared to actual BPD densities (total line length per unit volume), BPD etch pit densities (number per unit area) can be undercounted by a factor of 14 or greater for 4° offcut wafers[4]. Nevertheless, significant improvement in quality of p-type SiC wafers and further lowering of defect densities is necessary for development of devices such as n-channel IGBTs.

Synchrotron X-ray topography (XRT) is a powerful characterization technique widely applied in the semiconductor industry[5, 6]. High-resolution images of the internal structure of a crystal can be generated through X-rays generated by a synchrotron radiation source non-destructively. Both synchrotron white beam X-ray topography (SWBXT) and synchrotron monochromatic beam X-ray

This article is an open access article under the terms and conditions of the Creative Commons Attribution (CC BY) license
(https://creativecommons.org/licenses/by/4.0)

topography (SMBXT) are employed to obtain crystallographic defects and structural features. Transmission geometry and grazing incidence geometry are employed in SWBXT and SMBXT, respectively. Transmission geometry can expose the overall defect distribution, capturing defects throughout the crystal volume. Grazing incident geometry employs a very small incident angle (~2°) and penetrates the sample only to a shallow depth below the surface.

In this study, 6-inch high quality p-type 4H-SiC wafers are achieved by PVT method. The wafers were examined by SWBXT in transmission geometries and SMBXT in grazing incidence geometries to map the defect content and distribution.

Experimental

4° off-axis 150 mm PVT-grown 4H-SiC commercial wafers were imaged by synchrotron white beam X-ray topography (SWBXT) in transmission geometry at beamline 27-ID (HEX), National Synchrotron Light Source II at Brookhaven National Laboratory. Synchrotron monochromatic X-ray topography (SMBXT) in grazing incidence geometry images for samples was obtained at beamline 1-BM, Advanced Photon Source at Argonne National Laboratory. The energy of ~9.1KeV is used for SMBXT. As shown in Fig .1, X-ray beam enters one surface of the sample and exits from another surface in transmission geometry while X-ray incidences and exits sample from the same surface with an incident angle of ~2° in grazing incidence geometry. Images were recorded on the Agfa Structurix D3-SC films with resolution of ~1 μm for both geometries.

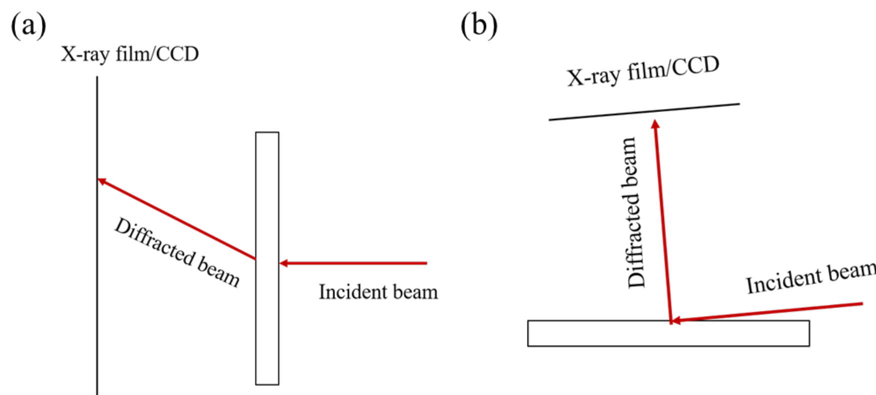

Fig. 1. Diagrams showing (a) transmission geometry, and (b) grazing incidence geometry for X-ray topography.

Results and Discussion

As shown in Fig. 2, the optical image of the high-quality p-type wafer exhibits a uniform blue color. Although such uniform coloration cannot be regarded as definitive proof of doping uniformity, it does qualitatively suggest a consistent distribution of aluminum dopants. Si face of the wafer is placed up. Facet is observed on the right side of the wafer with a darker blue color as marked by red arrows.

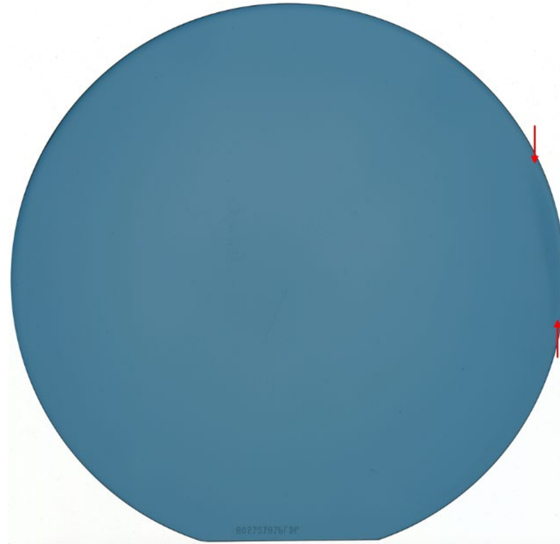

Fig. 2. Optical image of a high quality p-type wafer showing uniform blue color across the whole wafer. Facet is observed on the right side of the wafer and marked by red arrows.

The high quality p-type wafer is calculated to have average basal plane dislocation (BPD) density of ~$2.2*10^4$ cm^{-2}, threading screw dislocation (TSD) density of ~1331 cm^{-2}, and threading edge dislocation (TED) density of ~2163 cm^{-2}. Fig. 3 illustrates the procedure used to determine the dislocation densities across the entire wafer. As schematically shown by Fig. 3(a), 9 regions that are evenly distributed across the wafer are selected for density measurement. In each region, a grazing incidence image with $11\bar{2}8$ reflection as shown by Fig. 3(b) with size of 2.34mm x 1.75mm is acquired. The dislocation densities calculated from these images are then averaged to represent the overall density of the wafer. As marked by Fig. 3(b), in grazing incidence images, BPDs show linear white and black contrast, TSDs show large circular white contrast, and TEDs show small circular white or black contrast. The TSDs/TEDs number and total length of BPDs in each image can be manually counted. The densities of TSDs and TEDs are determined by dividing the total number of observed TSDs/TEDs by the image area (2.34 mm × 1.75 mm) while the density of BPDs is calculated by measuring the total length of BPD and normalizing by the imaged volume. Since the penetration depth of X-rays for grazing incidence geometry with $11\bar{2}8$ reflection is ~17μm. The volume where the BPDs are imaged is 2.34mm x 1.75mm x 17μm.

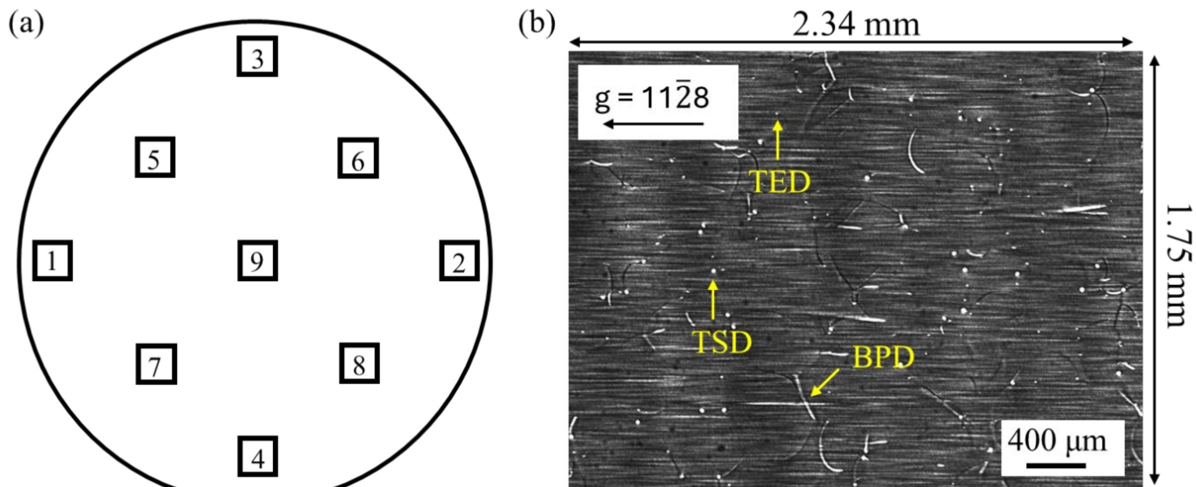

Fig. 3. (a) Schematic showing evenly distributed 9 regions across the wafer selected for dislocation density calculation. (b) Representative SMBXT grazing incidence image with $11\bar{2}8$ reflection acquired in each of the 9 regions for dislocation density evaluation.

In SWBXT transmission image, the low BPD density regions show whiter contrast compared to those with high BPD density regions. As marked by Fig. 4(a) in SWBXT transmission image for the whole p-type wafer, the middle ~12.6 cm diameter region is characterized by very low density of BPDs. Fig. 4(b)-4(d) shows the grazing incidence images that are obtained in the regions marked by box 1, 2, 3 in Fig. 4(a). The white horizontal linear contrasts in Fig. 4(b)-(d) are artifacts that are induced due to phase contrast effects from the beryllium window which serves as a vacuum barrier for the storage ring while permitting X-rays to pass into the beamline with minimal absorption. As indicated in Fig. 4(b), in addition to BPDs, TSDs, and TEDs, TSD pairs are observed as marked by red arrows suggesting nucleation in form of pairs is one source of TSDs for p-type wafers. BPD density for box 1, 2, 3 is low in the range of 581-1123 cm^{-2}. In fact, the middle ~12.6 cm diameter region is characterized to have average BPD density of 598 cm^{-2}, TSD density of 1447 cm^{-2}, and TED density of 1592 cm^{-2}, on par or better than commercial 6-inch n-type wafers.

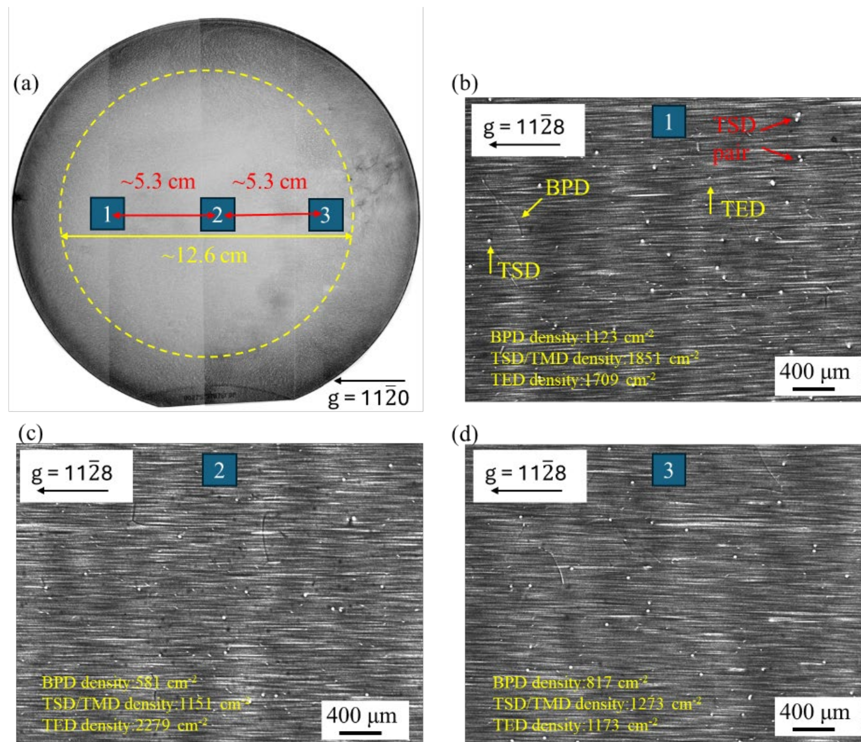

Fig. 4. (a) SWBXT image for the whole p-type wafer indicating the middle 12.6 cm region has low BPD density with whiter contrast, and (b)(c)(d) SMBXT grazing incidence geometry images with $11\bar{2}8$ reflection showing the low density dislocation regions in box 1, 2, 3 in (a).

The extent of prismatic slip for p-type wafer is vastly reduced compared to typical n-type wafers. Only the right periphery region of the wafer shows obvious prismatic slip dislocations contrast in SWBXT image. Other regions are free or have very low density of prismatic slip. As shown by Fig. 5. Prismatic slip dislocations have dark linear contrast along $[2\bar{1}\bar{1}0]$ and $[1\bar{2}10]$ directions in SWBXT transmission image as marked by yellow dashed line. Such orientations of the prismatic slip dislocations follow the predicted pattern by Guo et al[7, 8].

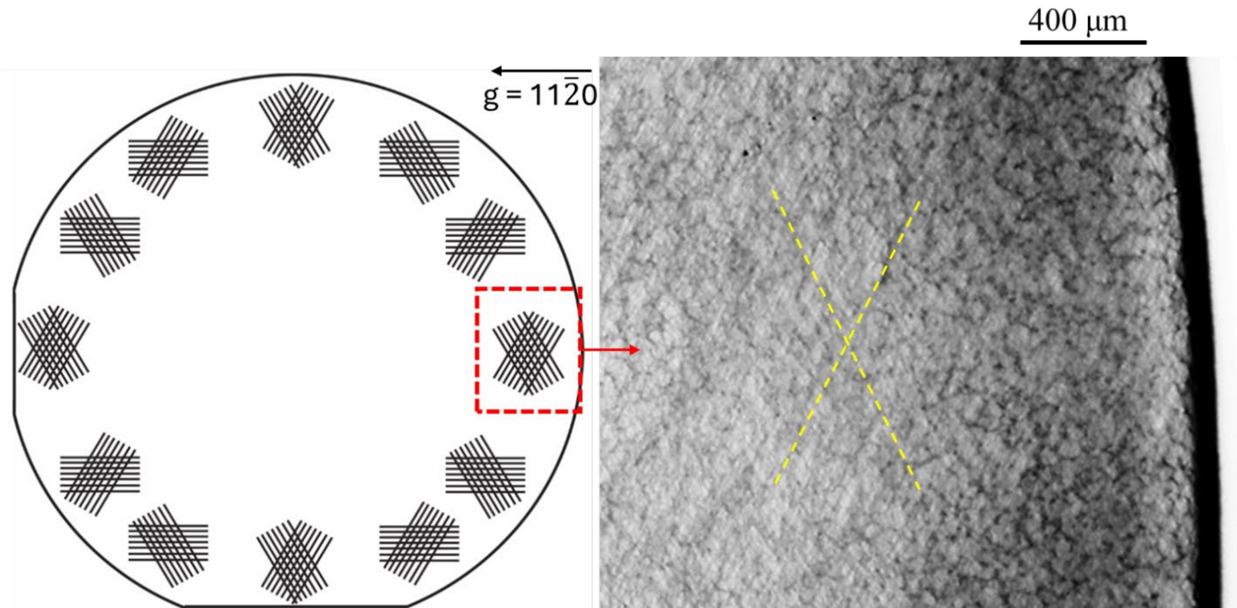

Fig. 5. SWBXT image with transmission geometry for the right periphery region of high quality p-type wafer showing distribution of prismatic slip. The orientation of prismatic slip dislocations follow the pattern predicted by Guo et al[7, 8].

Fig. 6 schematically marks the ranges of prismatic slip dislocations for a high quality p-type wafer and a commercial n-type wafer. The prismatic slip is observed only at the right ~1 cm periphery region for p-type wafer while at the whole periphery region with ~4.7cm range on the left and ~3.7cm range on the right for n-type wafer. Note that such observation emphasize the high quality that can be achieved in p-type wafers and does not imply that p-type doping in general results in lower prismatic slip dislocation densities than n-type doping.

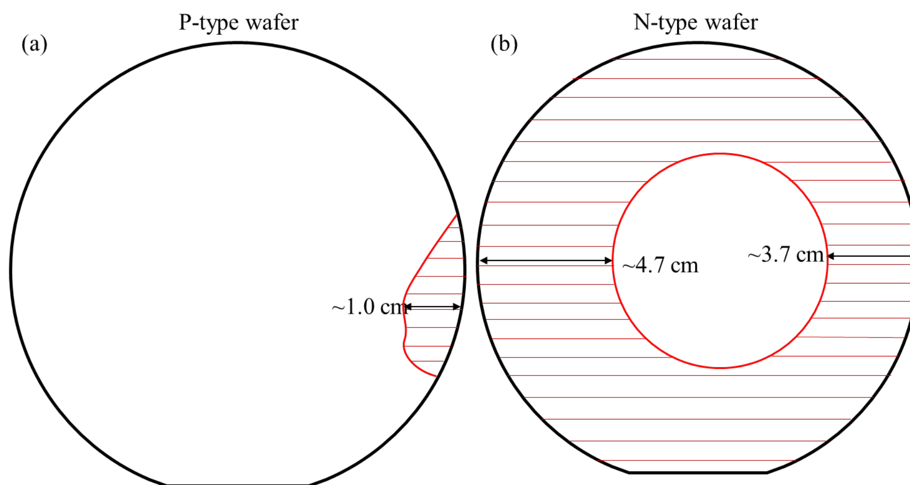

Fig. 6. Schematics showing distribution of prismatic slip for (a) p-type wafer, and (b) n-type wafer. Shaded red lines mark the region where prismatic slip is observed.

Summary

A 6-inch high quality p-type 4H-SiC wafer was achieved by PVT method with stable and uniform Al doping. Synchrotron X-ray topography images indicate on par or better quality than commercial 6-inch n-type wafers with BPD density ~$2.2*10^4$ cm^{-2}, TSD density ~1331 cm^{-2}, and TED density ~2163 cm^{-2}. Especially, the middle 12.6 cm diameter region has even lower BPD density of 598 cm^{-2}. Prismatic slip dislocations are only observed at right ~1.0cm periphery region of the wafer, vastly reduced compared to typical n-type wafers.

Acknowledgement

This work was supported by Pallidus, Inc.. This research used resources of the National Synchrotron Light Source II, a U.S. Department of Energy (DOE) Office of Science User Facility operated for the DOE Office of Science by Brookhaven National Laboratory under Contract No. DE-SC0012704. This research used resources of the Advanced Photon Source (Beamline 1-BM), a U.S. Department of Energy (DOE) Office of Science User Facility operated for the DOE Office of Science by Argonne National Laboratory under Contract No. DE-AC02-06CH11357. The Joint Photon Sciences Institute at SBU provided partial support for travel and subsistence for access to Advanced Photon Source.

References

[1] L. Han, L. Liang, Y. Kang, Y. Qiu, A review of SiC IGBT: models, fabrications, characteristics, and applications, TPEL. 36 (2021) 2080-2093.

[2] H. Suo, K. Eto, T. Ise, Y. Tokuda, H. Osawa, H. Tsuchida, T. Kato, H. Okumura, Crystal growth and evaluation of nitrogen and aluminum co-doped N-type 4H-SiC grown by physical vapor transport, J. Cryst. Growth. 498 (2018) 224-229.

[3] G. Wang, D. Sheng, Y. Yang, Z. Zhang, W. Wang, H. Li, Wafer-scale p-Type SiC single crystals with high crystalline quality, Cryst. Growth Des. 24 (2024) 5686-5692.

[4] H. Wang, S. Sun, M. Dudley, S. Byrappa, F. Wu, B. Raghothamachar, G. Chung, E. K. Sanchez, S. G. Mueller, D. Hansen, Quantitative comparison between dislocation densities in offcut 4H-SiC wafers measured using synchrotron x-ray topography and molten KOH etching, J. Electron. Mater. 42 (2013) 794-798.

[5] B. Raghothamachar, M. Dudley, G. Dhanaraj, X-ray topography techniques for defect characterization of crystals, in: G. Dhanaraj, K. Byrappa, V. Prasa, M. Dudley (Eds.), Springer Handbook of Crystal Growth, Springer, 2010, pp. 1425-1451.

[6] B. K. Tanner, D. K. Bowen, Characterization of Crystal Growth Defects by X-ray Methods, Springer Science & Business Media, New York, 2013.

[7] J. Guo, Y. Yang, B. Raghothamachar, J. Kim, M. Dudley, G. Chung, E. Sanchez, J. Quast, I. Manning, Prismatic slip in PVT-grown 4H-SiC crystals, J. Electron. Mater. 46 (2017) 2040-2044.

[8] J. Guo, Y. Yang, O. Y. Goue, B. Raghothamachar, M. Dudley, Study on the role of thermal stress on prismatic slip of dislocations in 4H-SiC crystals grown by PVT method, ECST 75 (2016) 163-168.